Contribution from the Department of Chemistry,
University of Missouri—Columbia, Columbia, Missouri 65211

Late-Transition-Metal μ-Oxo and μ-Imido Complexes. 8.[1] Rhodium Imido/Amido Coupling Reactions with Carbon Monoxide

Yuan-Wen Ge and Paul R. Sharp*

Received August 12, 1991

Treating tautomeric mixtures of $Rh_2(\mu\text{-NR})(CO)_2(\mu\text{-dppm})_2$ and $Rh_2(\mu\text{-NHR})(CO)_2(\mu\text{-dppm-H})(\mu\text{-dppm})$ (dppm = bis(diphenylphosphino)methane, dppm-H = bis(diphenylphosphino)methanide) (**1**/**2**) or $Rh_2(\mu\text{-NHMe})(CO)_2(\mu\text{-dppm-H})(\mu\text{-dppm})$ (**2**; R = Me) in CH_2Cl_2 or benzene with 1 equiv of CO gives $Rh_2(\mu\text{-}\eta^1\text{:}\eta^1\text{-RNCO})(CO)_2(\mu\text{-dppm})_2$ (**3**; R = Me, Ph, *p*-MePh, *p*-FPh, *p*-BrPh). Excess CO gives $Rh_2(\mu\text{-CO})(CO)_2(\mu\text{-dppm})_2$, RNCO, and $(RNH)_2CO$ (R = Ph, *p*-MePh, *p*-MeOPh, *p*-BrPh, *p*-FPh, *o*-MePh) or $Rh_2[\mu\text{-}\eta^1\text{:}\eta^1\text{-C(O)N(Me)C(O)}](\mu\text{-CO})(CO)_2(\mu\text{-dppm})_2$ (**4**) and $Rh_2(\mu\text{-CO})(CO)_2(\mu\text{-dppm})_2$ (R = Me). An X-ray crystal structure determination of **4** shows a "cradle" geometry with bridging cis phosphines and a dimetallacycloimide structure formed by insertion of CO into both Rh–N bonds. Crystals from CH_2Cl_2 are triclinic ($P\bar{1}$) with a = 12.117 (3) Å, b = 20.344 (4) Å, c = 11.160 (3) Å, α = 98.53 (2)°, β = 102.21 (2)°, γ = 91.21 (2)°, V = 2655.1 (2) Å^3, and Z = 2. Spectroscopic data indicate the formation of small amounts of the analogues of **4** (R = Ph, *p*-MePh, *p*-MeOPh, *p*-BrPh, *p*-FPh) at 2 atm of CO pressure and larger amounts at 35 atm. Treating $Rh_2(\mu\text{-}\eta^1\text{:}\eta^1\text{-RNCO})(CO)_2(\mu\text{-dppm})_2$ (**3**; R = *p*-FPh) with *p*-MePhNCO under a CO atmosphere gives a mixture of ureas, $[(p\text{-MePh})NH]_2CO$, $(p\text{-MePh})NHCOHN(p\text{-FPh})$, and $[(p\text{-FPh})NH]_2CO$.

Introduction

The catalytic carbonylation of nitro compounds to isocyanates is a potentially important industrial process (eq 1). Work on the

$$RNO_2 + 3CO \rightarrow RNCO + 2CO_2 \qquad (1)$$

catalytic reactions and on model systems has led to the suggestions of metal–imido (Scheme I) and/or metallacyclic (Scheme II) intermediates.[2] Although, on the basis of some of our own work on the carbonylation of rhodium nitrosobenzene complexes,[3] we favor metallacyclic intermediates, our synthesis of reactive imido complexes[4] as homogeneous models for late-transition-metal surface species gave us the opportunity to test the possible intermediacy of imido complexes in the catalytic cycle. This paper describes the full details[5] of our results from the reaction of our dppm (dppm = bis(diphenylphosphino)methane) Rh A-frame imido complexes, **1**, or their tautomers, the amido–methanide complexes, **2**. In most cases, **1** and **2** are in equilibrium (eq 2) with the equilibrium mixtures designated as **1**/**2**.[4a]

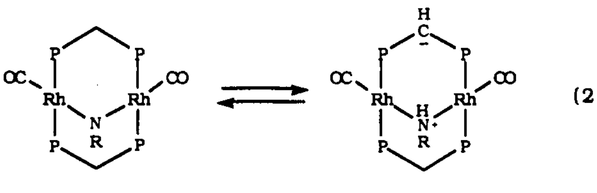

1 **2**

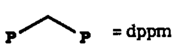

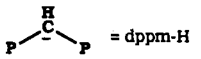

We find facile reactions with CO for a wide range of R. In most cases, the first equivalent of CO gives a coordinated isocyanate, as required for an imido intermediate in the catalytic cycle. Further reaction with CO does produce, in some cases, free isocyanate. However, the major products are ureas and dimetallacycloimide complexes, demonstrating some of the problems that may be encountered in catalytic reactions producing isocyanates, independent of the pathway leading to the isocyanates.

Scheme I

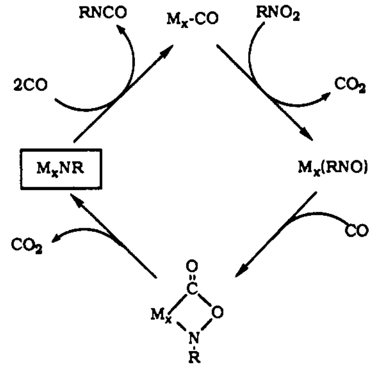

Scheme II

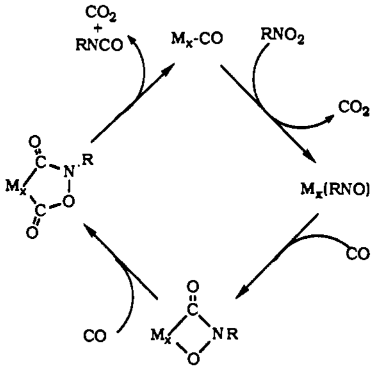

Results

Isocyanate Complexes. The addition of 1 equiv of CO to **1**/**2** (R = Ph, *p*-MePh, *p*-FPh, *p*-BrPh) or **2** (R = Me) at ambient temperatures leads to the formation of blue or purple (R = *p*-BrPh) products identified as the isocyanate A-frame complexes $Rh_2(\mu\text{-}\eta^1\text{:}\eta^1\text{-RNCO})(CO)_2(\mu\text{-dppm})_2$ (**3**) (eq 3; R = Me, Ph,

1/2 or **2** + CO ⟶

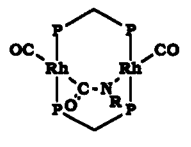

(3)

3

---

[1] Part 7: Li, W.; Barnes, C. L.; Sharp, P. R. *J. Chem. Soc., Chem. Commun.* **1990**, 1634–1636.

[2] (a) Leconte, P.; Metz, F.; Mortreaux, A.; Osborn, J. A.; Paul, F.; Petit, F.; Pillot, A. *J. Chem. Soc., Chem. Commun.* **1990**, 1616–1617. (b) Kunin, A. J.; Noirot, M. D.; Gladfelter, *J. Am. Chem. Soc.* **1989**, *111*, 2739. (c) Hwan Han, S.; Geoffroy, G. L. *Polyhedron* **1988**, *7*, 2331. (d) Hwan Han, S.; Song, J. S.; Macklin, P. D.; Nguyen, S. T.; Geoffroy, G. L. *Organometallics* **1989**, *8*, 2127–2138 and references cited therein. (e) Bhaduri, S.; Khwaja, H.; Sapre, N.; Sharma, K.; Basu, A.; Jones, P. G.; Carpenter, G. *J. Chem. Soc., Dalton Trans.* **1990**, 1313 and references cited therein. (f) Alessio, E.; Mestroni, G. *J. Organomet. Chem.* **1985**, *291*, 117. (g) Cenini, S.; Crotti, C.; Pizzoti, M.; Porta, F. *J. Org. Chem.* **1988**, *53*, 1243. (h) Bassoli, A.; Rindone, B.; Tollari, S.; Cenini, S.; Crotti, C. *J. Mol. Catal.* **1990**, *60*, 155–163. (i) L'-Eplattenier, F.; Matthys, P.; Calderazzo, F. *Inorg. Chem.* **1970**, *9*, 342. (j) Iqbal, A. F. M. *J. Org. Chem.* **1972**, *37*, 2792.

[3] Hoard, D. W. Unpublished work.

[4] (a) Ge, Y.-W.; Peng, F.; Sharp, P. R. *J. Am. Chem. Soc.* **1990**, *112*, 2632–2640. (b) Ramamoorthy, V.; Sharp, P. R. *Inorg. Chem.* **1990**, *29*, 3336.

[5] This work has appeared as a preliminary communication: Sharp, P. R.; Ge, Y.-W. *Organometallics* **1988**, *7*, 2234–2236.

0020-1669/92/1331-0379$03.00/0

Table I. Spectroscopic Data (IR, ^{1}H NMR, and ^{31}P{^{1}H} NMR) for the Isocyanate Complexes, **3**^{a}

R	$\nu_{CO}{}^b$	$\delta(CH_2)^c$	$\delta(CH_3)$	δ(Ph)	δ(P)(J)^d
Me	1963 vs	3.41	1.78	7.9–6.7	24.6 (143)
	1949 s^e	3.17			22.6 (174)^g
Ph	1963 vs	3.71		7.9–6.0	23.7 (130)
	1945 s	3.03			21.2 (169)
p-MePh	1963 vs	3.69	2.09	7.8–6.2	23.9 (132)
	1945 s	3.07			21.4 (172)
p-FPh	1966 vs	3.83		6.20 (9 Hz)^f	23.8 (129)
	1946 s	3.00		6.8–8.1	21.3 (169)
p-BrPh	1966 vs	3.78		6.00 (7 Hz)^f	23.3 (131)
	1948 s	3.00		6.8–8.1	20.8 (170)

^{a}All spectra were obtained at 22 ± 5 °C unless otherwise stated. ^{b}cm^{-1}; CH_2Cl_2. ν_{CO} bands for the RNCO ligand were not detected in CH_2Cl_2. Weak bands that could be due to the RNCO ligand were observed in mineral oil mulls for R = Me (see note *e*). ^{c}C_6D_6/CD_2Cl_2. ^{d}In CH_2Cl_2/C_6D_6 or CD_2Cl_2 unless otherwise stated. At 121 MHz, the spectra appear as a pair of doublets of multiplets (see text). The central shift of each doublet is given with *J* as the doublet spacing, in hertz. Simulations suggest $J \sim {}^1J_{RhP}$. ^{e}Mineral oil mull: 1954 sh, 1938 s, 1584 w, 1570 w cm^{-1}. ^{f}Triplet at 90 MHz. ^{g}Toluene-d_8.

p-MePh, *p*-FPh, *p*-BrPh). Qualitatively, the rate of the reaction depends on the R group and the solvent (CH_2Cl_2 > benzene). The formation of **3** slows as the electron-donating properties of the R groups decrease and finally stops for **1** when R = *p*-NO_2Ph. Heating the *p*-NO_2Ph complex under CO does give a reaction, but no isocyanate products are formed (vide infra). Complexes **1/2** with the more crowded R = *o*-MePh and *o,o'*-Me_2Ph react rapidly with 1 equiv of CO, but if the isocyanate complexes are formed, they must be transient intermediates and are not detected.

Solid samples of **3** can be isolated for R = Me, *p*-FPh, and *p*-BrPh by solvent removal in vacuo. However, attempts to isolate solid samples of **3** for R = Ph and *p*-MePh invariably lead to decomposition. Solutions of **3** for all R are unstable on prolonged standing, usually showing signals in the ^{31}P NMR spectra for $Rh_2(\mu\text{-}CO)(CO)_2(\mu\text{-dppm})_2$.[6] Crystals of **3** (R = *p*-FPh) can be grown by cooling concentrated CH_2Cl_2 reaction mixtures. Unfortunately, the crystals rapidly (seconds) disintegrate on exposure to a solvent-free atmosphere.

The η^1:η^1 geometry for **3** is assigned on the basis of the spectroscopic data (Table I). Thus, an AA'BB'XX' pattern is observed in the ^{31}P{^{1}H} NMR spectra. At low field strengths (90 MHz, proton) the pattern is very complex and asymmetric. However, at high field strengths (300 MHz, proton) the pattern is much simpler and appears as a double doublet of multiplets.

The ^{1}H NMR spectra are typical of dppm A-frame complexes and show two methylene signals indicative of equivalent methylenes in an A-frame structure.[7] The trans,trans-diphosphine A-frame geometry is also indicated by the observation of one major ν_{PC} band in the mineral oil mull IR spectrum of **3** (R = Me).[8]

When ^{13}CO is used for the preparation of **3** (R = Ph), the ^{13}C NMR spectra show the ^{13}C label scrambled over all three carbonyl sites (the two terminal CO ligands and the RNCO ligand). (In addition, remaining **1/2** is ^{13}CO enriched.) The terminal CO ligands of **3** show clear doublet-of-triplet patterns due to coupling to two P nuclei and one Rh nucleus. The isocyanate CO is an overlapping doublet of triplets due to weaker coupling to the Rh nucleus. With ^{15}N enrichment and ^{13}CO, the ^{13}C NMR spectrum of **3** (R = Ph) shows small single-bond ^{13}C–^{15}N coupling to the isocyanate carbon and larger coupling to one of the terminal CO ligands which we assign as trans to the isocyanate N (two-bond coupling).[9] The smallest coupling is to one of the terminal CO ligands which we assign as trans to the isocyanate carbon (three-bond coupling).

Table II. Organic Products from CO (2 atm) Reactions

R	RNCO^a	(RNH)$_2$-CO^b	R	RNCO^a	(RNH)$_2$-CO^b
Me	0		*p*-BrPh	0	90
p-MePh	25	50	*p*-NO_2Ph^c	0	0
Ph	6	75	*o*-MePh	33	7
p-MeOPh	15	40	*o,o'*-Me_2Ph	0	*d*
p-FPh	0	80			

^{a}Yields determined by IR spectroscopy. ^{b}Yields determined by HPLC of MeOH-quenched reaction mixtures. ^{c}Only detected product was *p*-NO_2PhNH_2. ^{d}Solubility was too low to determine.

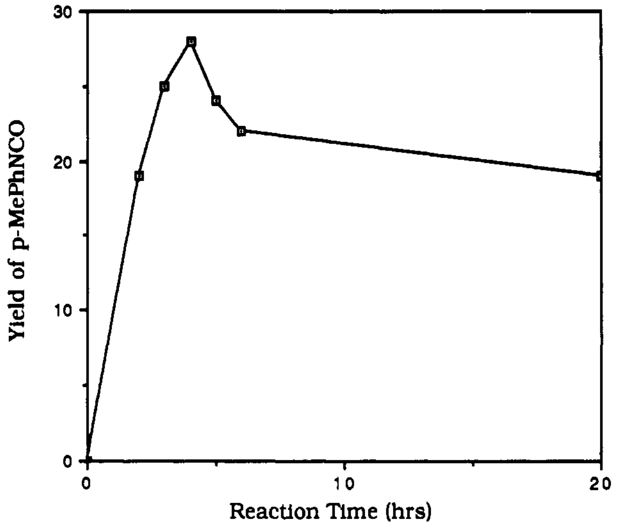

Figure 1. Yield of *p*-MePhNCO as a function of time for reaction 4.

Excess CO. Exposing **2** (R = Me) or **1/2** (R = Ph, *p*-MePh, *p*-FPh, *p*-MeOPh, *p*-BrPh) to 2 atm of CO at ambient temperatures gives **3** as the initial product (see eq 3).[10] Complex **3** reacts further with CO, again, qualitatively at a rate which slows as the R group becomes more electron withdrawing. The ortho-substituted phenyl complexes, **1/2** (R = *o*-MePh and *o,o'*-Me_2Ph) react similarly with CO at 2 atm and ambient temperatures but without evidence for the isocyanate complexes as intermediates. The final product distributions for these reactions vary according to the R group. For all but **2** (R = Me; vide infra), $Rh_2(\mu\text{-}CO)(CO)_2(\mu\text{-dppm})_2$ is the only major (at 2 atm of CO) metal-containing product (eq 4). The major organic products are

$$\mathbf{1/2}\ (R \neq Me) \xrightarrow{CO,\ 2\ atm} Rh_2(\mu\text{-}CO)(CO)_2(\mu\text{-dppm})_2 + \text{organics} \qquad (4)$$

the isocyanates, RNCO, and the ureas, $(RNH)_2CO$, in yields depending on the R group (Table II).

Several more experiments give information on the urea formation. When reaction 4 (R = *p*-MePh) is conducted in benzene, the formation of biphenyl is detected (~15% yield based on the urea), suggesting hydrogen atom abstraction as the source of the urea hydrogens. Treating the isocyanate complex **3** (R = *p*-FPh) with 1 equiv or more of (*p*-FPh)NCO under a nitrogen atmosphere rapidly produces the trimer [(*p*-FPh)NCO]$_3$. No or little [(*p*-FPh)NH]$_2$CO is produced. However, when the same experiment

---

(6) Woodcock, C.; Eisenberg, R. *Inorg. Chem.* **1985**, *24*, 1285. Woodcock, C.; Eisenberg, R. *Inorg. Chem.* **1984**, *23*, 4207–4211. Kubiak, C. P.; Woodcock, C.; Eisenberg, R. *Inorg. Chem.* **1982**, *21*, 2119.

(7) (a) Mague, J. T.; DeVries, S. H. *Inorg. Chem.* **1982**, *12*, 1632–1638 and references cited therein. (b) Jenkins, J. A.; Ennett, J. P.; Cowie, M. *Organometallics* **1988**, *7*, 1845–1853. (c) Balch, A. L.; Benner, L. S.; Olmstead, M. M. *Inorg. Chem.* **1979**, *18*, 2996–3003. (d) Brown, M. P.; Fisher, J. R.; Puddephatt, R. J.; Seddon, K. R. *Inorg. Chem.* **1979**, *18*, 2808–2813.

(8) Wu, J.; Fanwick, P. E.; Kubiak, C. P. *J. Am. Chem. Soc.* **1989**, *111*, 7812–7823.

(9) Second-order coupling larger than first-order coupling has been observed in organic compounds: Martin, G. J.; Martin, M. L.; Gouesnard, J.-P. *NMR, Basic Principles and Progress. 18. ^{15}N-NMR Spectroscopy*; Springer-Verlag: New York, 1981.

(10) Complex **3** was not characterized for R = *p*-MeOPh. However, the solutions of **1/2** (R = *p*-MeOPh) turn blue when exposed to CO, indicating the formation of **3**.

Table III. Crystallographic Data for $Rh_2[\mu\text{-}\eta^1{:}\eta^1\text{-}C(O)N(Me)C(O)](\mu\text{-}CO)(CO)_2(\mu\text{-dppm})_2\cdot CH_2Cl_2$ ($4\cdot CH_2Cl_2$)

formula	$C_{56}H_{47}NO_5P_4Rh_2\cdot CH_2Cl_2$	Z	2
a, Å	12.117 (3)	fw	1228.64
b, Å	20.344 (4)	space group	$P\bar{1}$ (No. 2)
c, Å	11.160 (3)	T, °C	22
α, deg	98.53 (2)	λ, Å	0.71069
β, deg	102.21 (2)	d_{calcd}, $g\cdot cm^{-3}$	1.54
γ, deg	91.21 (2)	μ(Mo Kα), cm^{-1}	8.80
V, Å^3	2655.1 (2)	$R(F_o)$[a]	0.030
		$R_w(F_o)$[b]	0.040

[a] $R(F_o) = (\sum||F_o| - |F_c||)/\sum F_o$. [b] $R_w(F_o) = [(\sum w(||F_o| - |F_c||)^2)/\sum wF_o^2]^{1/2}$; $w = 4F_o^2/(\sum F_o^2)^2$. Weights based on counting statistics were used. The weight modifier K in KF_o^2 is 0.001.

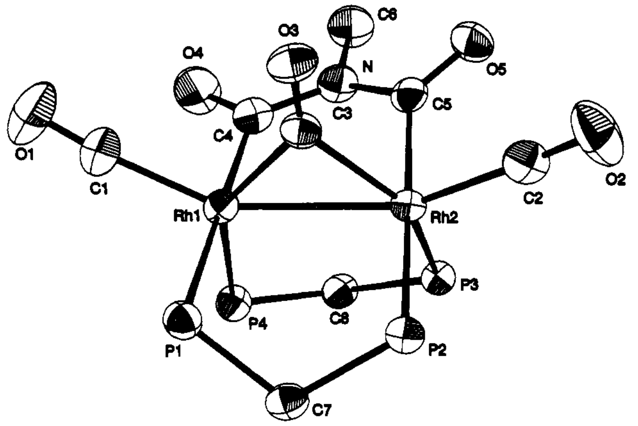

Figure 2. ORTEP plot of $Rh_2[\mu\text{-}\eta^1{:}\eta^1\text{-}C(O)N(Me)C(O)](\mu\text{-}CO)(CO)_2(\mu\text{-dppm})_2$ (**4**) (50% probability ellipsoids; phenyl rings omitted).

is repeated under a CO atmosphere, the urea is produced. A cross-coupling experiment with **3** (R = *p*-FPh) and 1.1 equiv of (*p*-MePh)NCO under a CO atmosphere produces a mixture of ureas containing both *p*-MePh and *p*-FPh groups. Monitoring the reaction of **1**/**2** (R = *p*-MePh) with CO by IR spectroscopy shows that the yield of isocyanate reaches a maximum when the solution is still blue (indicating the presence of **3**) and then declines to a stable value as the blue color fades. These data are presented in Figure 1. Finally, product distributions change with CO pressure. Increasing the CO pressure to 35 atm results in a sharp decrease in urea yield (R = *p*-MePh; vide infra).

As stated above, **1** (R = *p*-NO_2Ph) does not react with excess CO unless the reaction mixture is heated to 100 °C. The resulting products are the substituted aniline, *p*-NO_2PhNH_2, and $Rh_2(\mu\text{-}CO)(CO)_2(\mu\text{-dppm})_2$.

Dimetallacycloimide Complexes. The reaction of excess CO (2 atm) with **2** (R = Me) also gives $Rh_2(\mu\text{-}CO)(CO)_2(\mu\text{-dppm})_2$, but as the minor metal-containing product (33%). (The organic products derived from the lost CH_3N ligand have not been identified.) The major metal-containing product is the yellow dimetallacycloimide complex $Rh_2[\mu\text{-}\eta^1{:}\eta^1\text{-}C(O)N(Me)C(O)](\mu\text{-}CO)(CO)_2(\mu\text{-dppm})_2$ (**4**) (60%). The unique nature of **4** prompted an X-ray crystal structure determination.

Full crystallographic and structural data are included as supplementary material. Selected data are given in Tables III–V. An ORTEP drawing of the structure (without dppm phenyl rings) is given in Figure 2. The less common cis,cis-diphosphine geometry classifies **4** as a "cradle" complex.[8] The short Rh–Rh separation suggests the presence of a metal–metal bond. Neglecting the Rh–Rh bond, the geometry about each Rh is trigonal bipyramidal with the imide ligand and one dppm ligand in the axial positions and the other dppm and the CO ligands in the equatorial plane. The imide portion can be considered to result from the insertion of CO into the Rh–N bond of the isocyanate complex **3**. The distances in the non-metal portion of the ring are very similar to those found in the metallacycloimide complex $Cp_2W[C(O)N(Me)C(O)]$, obtained from Cp_2WCO and MeNCO.[11] The intra-ring angles are somewhat larger in **4** as a result of the larger ring size. The dimetallacycloimide portion is planar.

Table IV. Selected Coordinates for $Rh_2[\mu\text{-}\eta^1{:}\eta^1\text{-}C(O)N(Me)C(O)](\mu\text{-}CO)(CO)_2(\mu\text{-dppm})_2\cdot CH_2Cl_2$ ($4\cdot CH_2Cl_2$)

	x	y	z	B,[a] Å^2
Rh1	0.30915 (3)	0.213401 (18)	0.16922 (3)	2.174 (17)
Rh2	0.40056 (3)	0.329293 (17)	0.31259 (3)	1.936 (15)
P1	0.12456 (10)	0.23098 (6)	0.20625 (12)	2.42 (5)
P2	0.23421 (10)	0.35256 (6)	0.38708 (11)	2.11 (5)
P3	0.51277 (10)	0.27579 (6)	0.47493 (11)	2.18 (5)
P4	0.37390 (11)	0.14549 (6)	0.32643 (12)	2.46 (6)
O1	0.2287 (4)	0.13014 (22)	−0.0856 (4)	5.94 (23)
O2	0.4596 (3)	0.47799 (17)	0.3533 (4)	5.69 (25)
O3	0.3020 (3)	0.33565 (17)	0.0434 (3)	3.39 (17)
O4	0.4917 (3)	0.15016 (18)	0.0742 (4)	4.56 (19)
O5	0.6081 (3)	0.35815 (17)	0.2335 (3)	3.48 (17)
N	0.5559 (3)	0.24975 (19)	0.1808 (4)	2.80 (18)
C1	0.2546 (4)	0.1599 (3)	0.0107 (5)	3.44 (24)
C2	0.4394 (4)	0.42251 (24)	0.3410 (5)	3.00 (24)
C3	0.3204 (4)	0.30770 (23)	0.1303 (4)	2.48 (21)
C4	0.4695 (4)	0.20034 (23)	0.1350 (4)	2.54 (21)
C5	0.5373 (4)	0.31477 (25)	0.2331 (4)	2.61 (22)
C6	0.6676 (4)	0.2364 (3)	0.1545 (5)	3.8 (3)
C7	0.1316 (4)	0.28148 (23)	0.3572 (4)	2.33 (21)
C8	0.5042 (4)	0.18420 (23)	0.4327 (4)	2.58 (22)

[a] Anisotropic thermal parameters are given in the form of the isotropic equivalent displacement parameter defined as $(4/3)[a^2\beta(1,1) + b^2\beta(2,2) + c^2\beta(3,3) + ab(\cos\gamma)\beta(1,2) + ac(\cos\beta)\beta(1,3) + bc(\cos\alpha)\beta(2,3)]$.

Table V. Selected Intramolecular Distances (Å) and Angles (deg) for $Rh_2[\mu\text{-}\eta^1{:}\eta^1\text{-}C(O)N(Me)C(O)](\mu\text{-}CO)(CO)_2(\mu\text{-dppm})_2\cdot CH_2Cl_2$ ($4\text{-}CH_2Cl_2$)

Rh1–Rh2	2.7142 (9)	P2–C7	1.831 (5)
Rh1–P1	2.3837 (14)	P3–C8	1.848 (5)
Rh1–P4	2.4053 (14)	P4–C8	1.843 (5)
Rh1–C1	1.911 (5)	O1–C1	1.130 (6)
Rh1–C3	2.037 (5)	O2–C2	1.132 (6)
Rh1–C4	2.074 (5)	O3–C3	1.179 (6)
Rh2–P2	2.3686 (13)	O4–C4	1.207 (6)
Rh2–P3	2.4333 (14)	O5–C5	1.217 (6)
Rh2–C2	1.908 (5)	N–C4	1.394 (6)
Rh2–C3	2.039 (5)	N–C5	1.407 (6)
Rh2–C5	2.046 (5)	N–C6	1.466 (6)
P1–C7	1.823 (5)		
Rh2–Rh1–P1	93.90 (4)	P3–Rh2–C3	139.83 (13)
Rh2–Rh1–P4	94.83 (4)	P3–Rh2–C5	83.41 (13)
Rh2–Rh1–C1	151.38 (16)	C2–Rh2–C3	105.38 (20)
Rh2–Rh1–C3	48.28 (13)	C2–Rh2–C5	88.29 (20)
Rh2–Rh1–C4	85.39 (13)	C3–Rh2–C6	80.08 (18)
P1–Rh1–P4	98.45 (5)	Rh1–P1–C7	111.00 (15)
P1–Rh1–C1	93.84 (16)	Rh2–P2–C7	114.12 (15)
P1–Rh1–C3	90.26 (13)	Rh2–P3–C8	112.00 (15)
P1–Rh1–C4	178.51 (13)	Rh1–P4–C8	110.05 (15)
P4–Rh1–C1	111.18 (16)	C4–N–C5	123.3 (4)
P4–Rh1–C3	142.76 (14)	C4–N–C6	117.8 (4)
P4–Rh1–C4	82.91 (13)	C5–N–C6	118.1 (4)
C1–Rh1–C3	104.19 (21)	Rh1–C1–O1	175.1 (5)
C1–Rh1–C4	86.19 (21)	Rh2–C2–O2	177.1 (5)
C3–Rh1–C4	88.30 (18)	Rh1–C3–Rh2	83.51 (18)
Rh1–Rh2–P2	93.45 (4)	Rh1–C3–O3	138.9 (4)
Rh1–Rh2–P3	94.66 (4)	Rh2–C3–O3	137.1 (4)
Rh1–Rh2–C2	153.60 (15)	Rh1–C4–O4	121.6 (4)
Rh1–Rh2–C3	48.22 (13)	Rh1–C4–N	121.0 (3)
Rh1–Rh2–C5	86.61 (13)	O4–C4–N	117.5 (4)
P2–Rh2–P3	102.73 (5)	Rh2–C5–O5	124.4 (4)
P2–Rh2–C2	88.94 (15)	Rh2–C5–N	118.6 (3)
P2–Rh2–C3	95.35 (13)	O5–C5–N	116.9 (4)
P2–Rh2–C5	173.83 (14)	P1–C7–P2	112.24 (24)
P3–Rh2–C2	110.46 (15)	P3–C8–P4	117.26 (25)

The spectroscopic data for **4** are totally consistent with the solid-state structure. IR spectra show the terminal and bridging CO and imide ligand CO ligands in the expected regions. The

---

(11) Jernakoff, P.; Cooper, N. J. *J. Am. Chem. Soc.* **1987**, *109*, 2173–2174.

bands shift as expected on ^{13}C substitution. Two major ν_{PC} bands are observed in the solid-state IR spectrum consistent with the cis,cis-diphosphine geometry.[8] ^{1}H NMR spectra show four signals for the dppm methylenes, indicating two different types of dppm ligands with endo- and exo-methylene protons. ^{31}P NMR spectra show two well-separated signals for the two dppm ligands with complex non-first-order coupling. ^{13}C NMR spectra of **4** prepared from ^{13}CO show the downfield bridging CO and the higher field terminal CO ligands with relatively large Rh couplings. The imide carbons are in the same region as the terminal CO ligands, but with smaller Rh coupling.

An examination of the spectra of the reaction mixtures for the 2-atm CO reactions of **1**/**2** (R = *p*-MePh, *p*-FPh, *p*-MeOPh, *p*-BrPh) reveals the presence of small amounts of products with spectroscopic properties almost identical to those of **4**. We believe these products are the analogues of **4**. Increasing the CO reaction pressure to 35 atm increases the yield from traces to ~22% for R = *p*-MePh. At the same time, the yield of [(*p*-MePh)NH]$_2$CO decreases from 50 to 5% while the yield of (*p*-MePh)NCO increases from 25 to 35%.

Attempted Catalysis. Catalytic production of the isocyanate (and the urea) would be possible in this system if nitrobenzene would react with $Rh_2(\mu\text{-}CO)(CO)_2(\mu\text{-dppm})_2$ to re-form **1**/**2** (R = Ph). We tested this possibility by heating $Rh_2(\mu\text{-}CO)(CO)_2(\mu\text{-dppm})_2$ and nitrobenzene under a CO atmosphere. There is no reaction until about 80 °C, at which point the mixture turns black. No isocyanates are detected.

Discussion

The results presented above along with results from other groups[2d,12] demonstrate that isocyanates and/or isocyanate complexes can be formed from the reaction of CO with imido complexes. However, there are several features in our system which complicate matters. Since there is the tautomeric equilibrium between the imido complex **1** and the amido complex **2** for most, if not all, of the R groups, there is the possibility that the CO reactions occur via the imido tautomer, the amido tautomer, or both. In addition, while the formation of complexed isocyanate occurs readily, its release is apparently not so facile and further reactions may occur, leading to products resulting from the coupling of the coordinated isocyanate with either CO or free isocyanate.

Isocyanate Complexes. Two possible pathways to the isocyanate complexes are illustrated in Scheme III. Pathway A assumes that the imido tautomer **1** is the reacting species. In pathway B, the amido tautomer is the reacting species. On the basis of the ^{13}CO synthesis of **3** and the incorporation of ^{13}CO into unreacted **1**/**2**, there must be a rapid equilibrium involving CO coordination prior to N–C bond formation. This preequilibrium could involve **1** or **2**, since **1** and **2** are in rapid equilibrium, or both. We also know that the N–C bond formation is irreversible on the time scale of the reaction, since ^{13}CO is not incorporated into the RNCO ligand of **3** (R = *p*-FPh) on exposure to ^{13}CO. The C–N bond-forming step probably involves a nucleophilic attack of either an imido ligand from **1** or an amido ligand from **2** on a coordinated CO. (The qualitative dependence of the reaction rate on the electron-donating properties of the R group is consistent with nucleophilic attack.) Assuming that this step occurs at a bimetallic center and that ionic species are involved, as suggested by the greater rates in the more polar solvent, A and B would be the key intermediates in each case. These intermediates look particularly attractive, since the CO is coordinated to a cationic metal center and should be activated toward nucleophilic attack.[13] For B, the result of the C–N coupling is a carbamoyl group and proton transfer to the methanide gives the isocyanate complex. Though rare, CO coupling with amido ligands[14] and deprotonation of a carbamoyl complex[13b] (by an external base) are known processes. Additionally, the nucleophilic attacks can be viewed as analogous to amide (A = metallaamide) or amine (B = metallaamine) attacks on coordinated CO. Both of these processes have ample literature precedent.[15,16]

Scheme III

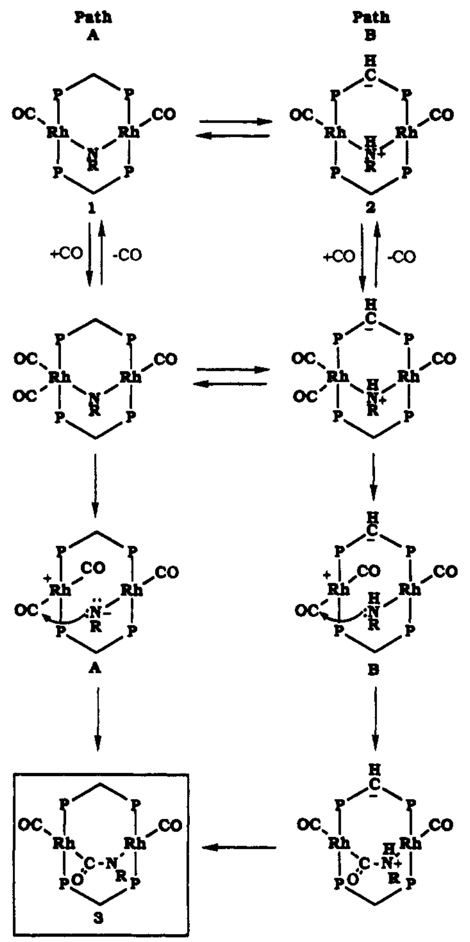

In an attempt to answer the question of which tautomer, **1** or **2**, is the reacting species, we treated the cationic amido complex, $[Rh_2(\mu\text{-}NHPh)(CO)_2(\mu\text{-dppm})_2]^+$, with CO. A rapid reaction did occur, and although we were unable to isolate any of the metal-containing products, PhNCO was formed in an 11% yield. This facile reaction implicates the amido tautomer and intermediate B. We also favor the amido tautomer intermediate B because of the expected ease of breaking a μ_2-amido–Rh bond. Because of the formal positive charge on the bridging amido ligand, breaking the bridge forms a neutral terminal amido ligand. The amido ligand with its lone pair electrons would be poised for the nucleophilic attack on the adjacent CO. On the other hand, breaking the imido bridge (heterolytically) results in a negative charge on the nitrogen which could not be readily delocalized. Alternatively, the process may be analogous to an alkyl group

---

(12) Glueck, D. S.; Hollander, F. J.; Bergman, R. G. *J. Am. Chem. Soc.* **1989**, *111*, 2719–2721.

(13) (a) Shen, J.-K.; Gao, Y.-C.; Shi, Q.-Z.; Basolo, F. *Organometallics* **1989**, *8*, 2144 and references cited therein. (b) Jetz, W.; Angelici, R. J. *J. Am. Chem. Soc.* **1972**, *94*, 3799–3802.

(14) (a) Fryzuk, M. D.; Montgomery, C. D. *Coord. Chem. Rev.* **1989**, *95*, 1–40. (b) Bryndza, H. E.; Tam, W. *Chem. Rev.* **1988**, *88*, 1163–1188. (c) Lappert, M. F.; Powers, P. P.; Sanger, A. R.; Srivastava, R. C. *Metal and Metalloid Amides: Synthesis, Structures, and Physical and Chemical Properties*; Ellis Horwood Ltd.: Chichester, U.K. 1980; pp 585–586. (d) Calet, S.; Urson, F.; Alper, H. *J. Am. Chem. Soc.* **1989**, *111*, 931–934. (e) Chisholm, M. H.; Hammond, C. E.; Huffman, J. C. *Organometallics* **1987**, *6*, 210–211. (f) Fagan, P. J.; Manriquez, J. M.; Vollmer, S. H.; Day, C. S.; Day, V. W.; Marks, T. J. *J. Am. Chem. Soc.* **1981**, *103*, 2206–2220.

(15) We thank a reviewer for pointing out this analogy.

(16) Angelici, R. J. *Acc. Chem. Res.* **1972**, *5*, 335. Brown, F. J. *Prog. Inorg. Chem.* **1980**, *27*, 1. Cardin, D. J.; Centikaya, B.; Lappert, M. F. *Chem. Rev.* **1972**, *72*, 545. Cardin, D. J.; Centikaya, B.; Doyle, M. J.; Lappert, M. F. *Chem. Soc. Rev.* **1973**, *2*, 99. Casey, C. P. *Transition Met. Organomet. Org. Synth.* **1976**, *1*, 190. Fischer, E. O. *Adv. Organomet. Chem.* **1976**, *14*, 1.

Scheme IV

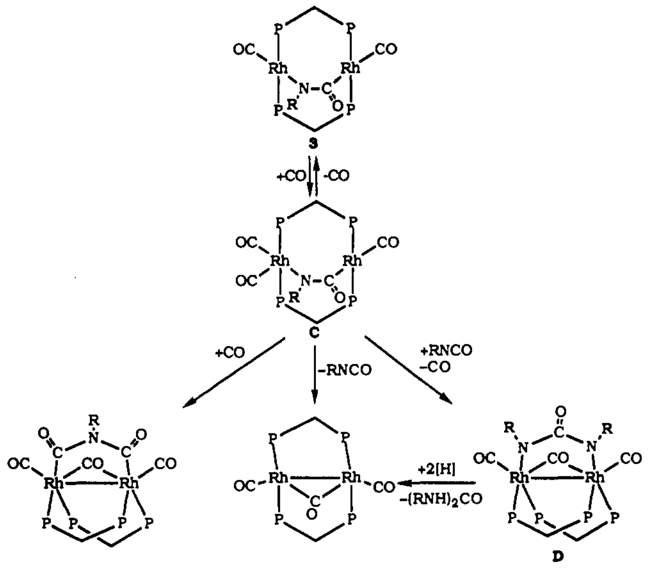

migration to coordinated CO with either the imido or amido ligand and may occur at a monometallic center.

The possible involvement of the amido tautomer **2** in the CO reactions is very interesting. Complex **2** represents an "imido equivalent". That is, the imido ligand is "protected" by protonation with the internal acid, PCH_2P. Following the CO insertion, the proton is removed by the internal conjugate base, $[PCHP]^-$, to give the product which would have resulted from the direct reaction of the imido ligand. This ability to transfer a proton is similar to some surface reactions where protons are transferred between adjacent surface sites during the catalytic cycle.[17]

Excess-CO Reactions. In the excess-CO reactions, the isocyanate complexes, **3**, are either detected intermediates or are probable transient intermediates. Again, a rapid preequilibrium must exist where CO reversibly coordinates to **3** (Scheme IV). This is detected by the exchange of the terminal CO ligands of **3** with ^{13}CO. The CO–isocyanate complex C then has three options. With the electron-rich MeNCO complex or with high CO pressures, CO inserts into the Rh–N isocyanate bond to give the dimetallacycloimide complexes **4** and its analogues). Alternatively, the RNCO ligand is displaced to give free isocyanate. As the free isocyanate concentration builds, isocyanate competes with CO for insertion into the Rh–N bond of the CO–isocyanate complex C and head-to-tail isocyanate coupling occurs. Decarbonylation would give a dimetallacyclourea complex D which is unstable and opens with abstraction of H atoms to form the observed ureas. The formation of biphenyl when the reaction is conducted in benzene is consistent with a hydrogen abstraction process. Net head-to-tail isocyanate coupling and decarbonylation to metallacycloureas have been observed in other systems.[18] It should also be noted that ureas are common coproducts in the catalytic reactions (eq 1).[2h,i]

Competition of CO and RNCO for complex C is consistent with the observed drop in the urea yield on increasing the CO pressure from 2 to 35 atm. The time dependency of the isocyanate yield (Figure 1) and the cross-coupling experiments indicate that the reaction of RNCO with complex C gives the ureas. An interesting question here is why CO (i.e. complex C) must be present for the urea-forming reaction to occur. One possibility is that complex C rearranges to another intermediate with a nonbridging isocyanate ligand, which is more reactive and more easily displaced.

Conclusions

Imido complexes (possibly via amido complexes in the present case) can couple, under mild conditions, with CO to form isocyanate complexes, thus demonstrating the viability of at least a portion of the catalytic cycle shown in Scheme I. However, isocyanate complexes, which are intermediates in both of the catalytic cycles (Schemes I and II), can be highly reactive. Reactions that compete with the required RNCO displacement could kill the catalyst (via the formation of imide complexes or stable urea complexes) or divert the product from RNCO to ureas.

Experimental Section

General Procedures. All experiments were performed under a dinitrogen atmosphere in a VAC drybox or by Schlenk techniques. Solvents were carefully dried under dinitrogen by recommended published techniques.[19] The petroleum ether used had a boiling range of 35–60 °C. $Rh_2(\mu\text{-NR})(CO)_2(\mu\text{-dppm})_2/Rh_2(\mu\text{-NHR})(CO)_2(\mu\text{-dppm-H})(\mu\text{-dppm})$ (**1/2**) and $Rh_2(\mu\text{-NHMe})(CO)_2(\mu\text{-dppm-H})(\mu\text{-dppm})$ (**2**; R = Me) were prepared according to literature procedures.[4a] $Li^{15}NHPh$, used for the preparation of ^{15}N-labeled **1/2** (R = Ph), was prepared from $LiN(SiMe_3)_2$ and $Ph^{15}NH_2$ (99%, Cambridge Isotopes) in petroleum ether/Et_2O. CP grade CO (Matheson) and ^{13}CO (99%, Monsanto Research Corp.) were used as received. The pressure reactions were conducted in a Fisher-Porter pressure bottle or, for the higher pressures, in a Parr reactor. NMR shifts are reported in ppm referenced to TMS for ^1H and ^{13}C and to external H_3PO_4 for ^{31}P. Microanalyses were performed (drybox) by Gailbraith Microanalytical Laboratories, Inc., or Oneida Research Services, Inc. HPLC analyses were preformed on MeOH-quenched (10/1) reaction mixtures using a 25-cm C_{18} reversed-phase microsorb column with 60/40 $MeOH/H_2O$ containing 0.1% nitric acid and a fixed-wavelength (254 nm) detector. Yields are based on calibration curves obtained from authentic samples.

Preparation of $Rh_2(\mu\text{-}\eta^1\text{:}\eta^1\text{-RNCO})(CO)_2(\mu\text{-dppm})_2$ (3; R = Me). Gaseous CO (1.84 mL, 0.076 mmol, 23 °C) was injected into a stirred solution of $Rh_2(\mu\text{-NHMe})(CO)_2(\mu\text{-dppm})(\mu\text{-dppm-H})$ (**2**; R = Me) (80 mg, 0.075 mmol) in CH_2Cl_2 (4 mL) in a closed 20-mL vial. The solution turned from orange to blue in 15 min. After 1 h, the solution was concentrated and Et_2O was added to precipitate a blue solid, which was filtered off, washed with Et_2O, and dried in vacuo to give 70 mg of $Rh_2(\mu\text{-}\eta^1\text{:}\eta^1\text{-MeNCO})(CO)_2(\mu\text{-dppm})_2$ (**3**) in 85% yield. Alternatively, reasonably pure samples may be isolated by solvent removal in vacuo.

Anal. Calcd (found) for $C_{54}H_{47}NO_3P_4Rh_2$: C, 59.6 (58.6); H, 4.4 (4.5); N, 1.3 (1.1). Occluded solvent is a common problem for the analysis of dppm A-frame compounds,[20] and residual CH_2Cl_2 accounts for the low C and low N analyses. With 0.4 equiv of CH_2Cl_2: C, 58.2 (58.6); H, 4.3 (4.5); N, 1.2 (1.1).

Preparation of $Rh_2(\mu\text{-}\eta^1\text{:}\eta^1\text{-RNCO})(CO)_2(\mu\text{-dppm})_2$ (3; R = *p*-FPh, *p*-BrPh). The procedure, using **1/2** (R = *p*-FPh, *p*-BrPh), was the same as for R = Me except hexane was used in place of Et_2O. Yields were ~90%. The reactions were slow especially for R = *p*-BrPh and required several hours to reach completion (^{31}P NMR monitoring). The *p*-BrPh complex is purple, and the *p*-FPh complex is blue.

Anal. Calcd (found) for $C_{59}H_{48}FNO_3P_4Rh_2$: C, 60.7 (60.9); H, 4.1 (4.2); N, 1.2 (1.3). The *p*-BrPh complex was difficult to obtain pure, frequently being contaminated with starting material or decomposition products. Analyses were not successful.

Observation of $Rh_2(\mu\text{-}\eta^1\text{:}\eta^1\text{-RNCO})(CO)_2(\mu\text{-dppm})_2$ (3; R = *p*-MePh, Ph). In a typical experiment, 1 equiv of gaseous CO was injected into a 0.7-mL CD_2Cl_2 solution of 40 mg of **1/2** in an NMR tube. With shaking, the solution turned from orange to blue. After 0.5 (*p*-MePh) to 1 h (Ph), the spectroscopic data were recorded. Removal of the solvent in vacuo or adding petroleum ether to precipitate the product gave an unidentified mixture of compounds.

^{13}C NMR for R = *p*-MePh (66 MHz, C_6D_6/CD_2Cl_2, ^{13}CO enriched): 205 (m, J_{RhC} = 17 Hz, J_{PC} = 9 Hz, *p*-MePhN*C*O), 201 (d of t, J_{RhC} = 57 Hz, J_{PC} = 13 Hz, CO), 195 (d of t, J_{RhC} = 64 Hz, J_{PC} = 15 Hz, CO′).

^{13}C NMR for R = Ph (66 MHz, C_6D_6/CD_2Cl_2, ^{13}CO and ^{15}N enriched): 206 (m, J_{RhC} = 18 Hz, J_{PC} = 9 Hz, J_{NC} = 9 Hz, PhN*C*O), 202 (dd of t, J_{RhC} = 57 Hz, J_{PC} = 13 Hz, J_{NC} = 4 Hz, CO trans to the PhNCO carbon), 195 (dd of t, J_{RhC} = 65 Hz, J_{PC} = 15 Hz, J_{NC} = 14 Hz, CO trans to the PhNCO nitrogen).

Reaction of 1/2 (R = *o*-MePh, *o*,*o*′-Me_2Ph) with 1 equiv of CO. The procedure was the same as above. However, no blue or purple color was observed. Spectroscopic examination of the orange reaction mixtures after 0.5 h revealed the formation of $Rh_2(\mu\text{-CO})(CO)_2(\mu\text{-dppm})_2$ and

---

(17) Madix, R. J.; Jorgensen, S. W. *Surf. Sci.* **1987**, *183*, 27–43 and references cited therein.

(18) For reviews of metal–organic isocyanate chemistry see: (a) Braunstein, P.; Nobel, D. *Chem. Rev.* **1989**, *89*, 1927–1945. (b) Cenini, S.; La Monica, G. *Inorg. Chim. Acta* **1976**, *18*, 279–293.

(19) Burfield, D. R.; Lee, K.-H.; Smithers, R. H. *J. Org. Chem.* **1977**, *42*, 3060–3065.

(20) Balch, A. L.; Benner, L. S.; Olmstead, M. M. *Inorg. Chem.* **1979**, *18*, 2996–3003.

other unidentified products (R = *o,o′*-Me_2Ph) with no remaining **1/2**. No free isocyanate was detected.

^{13}CO Exchange with $Rh_2(\mu\text{-}\eta^1:\eta^1\text{-RNCO})(CO)_2(\mu\text{-dppm})_2$ (3; R = *p*-FPh). Two milliliters of ^{13}CO was injected into a 20-mL vial containing **3** (R = *p*-FPh), prepared from 28 mg of **1/2** (R = *p*-FPh), and 1 mL of CH_2Cl_2. After 45 min, all volatiles were removed in vacuo. The solid was dissolved in 0.7 mL of CD_2Cl_2 for NMR analysis. The only CO signals observed in the ^{13}C NMR spectrum (66 MHz) of the blue solution were those for the terminal carbonyl ligands of **3**: 201 (d of t, J_{RhC} = 57 Hz, J_{PC} = 13 Hz, CO), 195 (d of t, J_{RhC} = 65 Hz, J_{PC} = 15 Hz, CO′).

Preparation of $Rh_2[\mu\text{-}\eta^1:\eta^1\text{-C(O)N(Me)C(O)}](\mu\text{-CO})(CO)_2(\mu\text{-dppm})_2$ (4). A stirred solution of $Rh_2(\mu\text{-NHMe})(CO)_2(\mu\text{-dppm})(\mu\text{-dppm-H})$ (**2**; R = Me) in CH_2Cl_2 was pressurized to 2 atm of CO. The solution rapidly turned blue, and after several hours, it became orange. After 20 h, the CO pressure was carefully released. IR and ^{31}P NMR analysis of the reaction mixture showed $Rh_2[\mu\text{-}\eta^1:\eta^1\text{-C(O)N(Me)C(O)}](\mu\text{-CO})(CO)_2(\mu\text{-dppm})_2$ (**4**) (~60%), $Rh_2(\mu\text{-CO})(CO)_2(\mu\text{-dppm})_2$ (~33%), $Rh_2(\mu\text{-OHCl})(CO)_2(\mu\text{-dppm})_2$ (~7%),[21] and an unidentified compound with an IR band at 2228 cm^{-1} (not MeNCO). The mixture was concentrated, and Et_2O was added to precipitate yellow $Rh_2(\mu\text{-}\eta^1:\eta^1\text{-C(O)-N(Me)C(O)}](\mu\text{-CO})(CO)_2(\mu\text{-dppm})_2$ (**4**). The mother liquor contained additional **4**, but no attempt was made to recover it. X-ray-quality crystals were grown from CH_2Cl_2/Et_2O.

IR (cm^{-1}, mineral oil): 1999 s, 1984 vs (terminal ν_{CO}), 1787 s (briding ν_{CO}), 1620 m, 1567 m (imide ν_{CO}), 1093 m, 994 m (cis ν_{PC}). The assignment of the ν_{CO} bands was based on shifts with ^{13}C substitution: 1954 s, 1940 vs (terminal $\nu_{^{13}CO}$), 1745 s (bridging $\nu_{^{13}CO}$), 1585 m, 1539 m (imide $\nu_{^{13}CO}$). ^1H NMR (300 MHz, CD_2Cl_2): 7.67–6.67 (m, 40, Ph), 3.98, 3.54, 3.16, 2.59 (m, 1 each, CH_2), 2.09 (s, 3, CH_3). ^{13}C NMR (66 MHz, CD_2Cl_2, ^{13}CO enriched): 241 (quint of t, $J_{RhC} = J_{PC}$ = 42 Hz, J_{PC} = 11 Hz, μ-CO), 191 (m, imide CO), 190 (d of t, J_{RhC} = 77 Hz, J_{PC} = 10 Hz, terminal CO). ^{31}P NMR (121 MHz, CD_2Cl_2): 31.8 and 15.1 (m, P and P′).

Reactions of 1/2 (R = *p*-MePh, Ph, *p*-FPh, *p*-BrPh, *p*-MeOPh, *o*-MePh, *o,o′*-Me_2Ph) with Excess CO (2 atm). In a typical experiment, 40 mg of the imido/amido complex **1/2** was dissolved in 2 mL of CH_2Cl_2 and the solution was placed under 2 atm of CO. Initially, the mixtures turned blue or purple (R ≠ *o*-MePh, *o,o′*-Me_2Ph), and after several hours, they became orange. After 20 h, the pressure was carefully released and the solution was analyzed, first by IR and ^{31}P NMR spectroscopy and then by HPLC (after quenching with ~20 mL of MeOH). IR and ^{31}P NMR spectra showed $Rh_2(\mu\text{-CO})(CO)_2(\mu\text{-dppm})_2$ as the major metal product in all cases. The IR spectra also showed weak bands due to $Rh_2[\mu\text{-}\eta^1:\eta^1\text{-C(O)N(R)C(O)}](\mu\text{-CO})(CO)_2(\mu\text{-dppm})_2$ (R = Ph, *p*-MePh, *p*-FPh, *p*-BrPh, *p*-MeOPh), analogues of **4**, and unidentified bands for R = *o*-MePh and *o,o′*-Me_2Ph. Free-isocyanate yields were obtained from the absorbance of the isocyanate bands in the IR spectra. Urea yields were obtained from the HPLC analyses. Yields of the organic products are given in Table II. The urea $[(o,o'\text{-}Me_2Ph)NH]_2CO$ could not be quantified because of its poor solubility.

Reaction of 1/2 (R = *p*-MePh) with Excess CO (35 atm). A stirred solution of **1/2** (R = *p*-MePh; 20 mg, 0.018 mmol) in 1 mL of CH_2Cl_2 was placed under 35 atm of CO. After 5 h, the pressure was carefully released and the solution was analyzed as described above. IR spectra (CH_2Cl_2) showed, in addition to *p*-MePhNCO and $Rh_2(\mu\text{-CO})(CO)_2(\mu\text{-dppm})_2$, strong bands for $Rh_2[\mu\text{-}\eta^1:\eta^1\text{-C(O)N(}p\text{-MePh)C(O)}](\mu\text{-CO})(CO)_2(\mu\text{-dppm})_2$ at 1991 s, 1790 m, 1620 m, and 1586 m cm^{-1}. ^{31}P NMR spectra (36 MHz, CH_2Cl_2), with integration, showed $Rh_2(\mu\text{-CO})(CO)_2(\mu\text{-dppm})_2$ (~70%), $Rh_2[\mu\text{-}\eta^1:\eta^1\text{-C(O)N(}p\text{-MePh)C(O)}](\mu\text{-CO})(CO)_2(\mu\text{-dppm})_2$ (31 (m) and 15 (m)) (~22%), and other unidentified peaks (~8%). The yield (IR) of free isocyanate, (*p*-MePh)NCO, was 35%. The yield of urea, $[(p\text{-MePh})NH]_2CO$, was 5%.

Reaction of $[Rh_2\{\mu\text{-NH(}p\text{-MePh)}\}(CO)_2(\mu\text{-dppm})_2]SO_3CF_3$ with CO. An orange solution of $[Rh_2\{\mu\text{-NH(}p\text{-MePh)}\}(CO)_2(\mu\text{-dppm})_2]SO_3CF_3$ (32 mg, 0.028 mmol) in 1 mL of CH_2Cl_2 was stirred under 2 atm of CO. The solution turned red. IR analysis of the reaction mixture showed the formation of (*p*-MePh)NCO (2279 cm^{-1}, 11%) and other unidentified products with CO bands at 2001 sh, 1989 vs, 1898 w, and 1872 w cm^{-1}. ^{31}P NMR data suggested a complex mixture.

Reaction of $Rh_2(\mu\text{-}\eta^1:\eta^1\text{-RNCO})(CO)_2(\mu\text{-dppm})_2$ (3; R = *p*-FPh) with Isocyanates. A. (*p*-FPh)NCO. $Rh_2(\mu\text{-}\eta^1:\eta^1\text{-}p\text{-FPhNCO})(CO)_2(\mu\text{-dppm})_2$ (20 mg, 0.017 mmol) in 1 mL of CH_2Cl_2 was treated with excess (*p*-FPh)NCO (10 μL, 1.056 g/mL, 0.016 mmol). After 20 h, the solution had changed from purple to brown and the isocyanate was all consumed. IR (cm^{-1}, CH_2Cl_2): 1982 vs, 1966 s, 1941 m, 1721 sh, 1717 s. The ^{31}P NMR spectrum was complicated. When hexane was added, a solid precipitated. The solid was filtered off, dried, and extracted with Et_2O to give an orange solution. Allowing the solution to stand at −40 °C for 2 weeks gave colorless crystals identified as the isocyanate trimer, $(RNCO)_3$. IR (cm^{-1}, CH_2Cl_2): 1721 sh, 1717 vs. The same results, but with a smaller yield of the trimer, were obtained with 1 equiv of (*p*-FPh)NCO.

B. (*p*-FPh)NCO and CO. The same reaction as in part A was conducted under 2 atm of CO. IR, ^{31}P NMR, and HPLC analyses indicated the formation of $Rh_2(\mu\text{-CO})(CO)_2(\mu\text{-dppm})_2$, $[(p\text{-FPh})NH]_2CO$, and $[(p\text{-FPh})NCO]_3$.

C. *p*-MePhNCO and CO. $Rh_2(\mu\text{-}\eta^1:\eta^1\text{-(}p\text{-FPh)NCO})(CO)_2(\mu\text{-dppm})_2$ in CH_2Cl_2 was treated with *p*-MePhNCO under 2 atm of CO. After 18 h, the solution was orange. IR, ^{31}P NMR, and HPLC analyses showed the presence of remaining *p*-MePhNCO, $[p\text{-MePhNCO}]_3$, $Rh_2(\mu\text{-CO})(CO)_2(\mu\text{-dppm})_2$, and a mixture of the three ureas, $[(p\text{-FPh})NH]_2CO$, (*p*-FPh)NHCONH(*p*-MePh), and $[(p\text{-MePh})NH]_2CO$ (ratio 1/4/2.7, assuming equal response on the HPLC detector).

Structure Analyses. An outline of crystallographic and data collection parameters is given in Table III. Yellow, prismatic crystals of **4** were grown from CH_2Cl_2. A crystal was selected (0.10 × 0.17 × 0.27 mm) in air and mounted in a capillary containing an atmosphere saturated in CH_2Cl_2. (The crystals are unstable to solvent loss.) Details of the data collection and reduction and the structure solution and refinement are provided as supplementary material.

Acknowledgment. We thank the Petroleum Research Fund, administered by the American Chemical Society, ARCO Chemical Co., Johnson Matthey (loan of $RhCl_3$), and the Division of Chemical Sciences, Office of Basic Energy Sciences, Office of Energy Research, U.S. Department of Energy (Grant DE-FE02-88ER13880), for support of this work. The National Science Foundation provided a portion of the funds for the purchase of the X-ray (Grant CHE-7820347) and NMR (Grant PCM-8115599) equipment. We are grateful to Professors E. Maatta and R. Angelici for helpful discussions.

Supplementary Material Available: A figure showing the ^{31}P NMR spectra of **3** and tables of crystallographic and data collection parameters, positional parameters, thermal parameters, torsion angles, dppm bond distances and angles, and least-squares planes for **4** (11 pages); a listing of structure factors for **4** (25 pages). Ordering information is given on any current masthead page.

---

(21) Deraniyagala, S. P.; Grundy, K. R. *Inorg. Chem.* **1985**, *24*, 50–56.